JOURNAL OF MATERIALS SCIENCE 35 (2000) 4465–4476

An investigation of brittle fracture of composite insulator rods in an acid environment with either static or cyclic loading

S. H. CARPENTER, M. KUMOSA
Center for Advanced Materials and Structures, University of Denver, 2450 S. Gaylord St., Denver, CO 80208
E-mail: mkumosa@du.edu

The effect of static and cyclic loading conditions on the stress corrosion cracking of unidirectional glass reinforced polymer (GRP) rods used in composite high voltage insulators has been investigated. A series of stress corrosion experiments has been performed on unidirectional E-glass/modified polyester composite rods. The rods have been subjected to mechanical tensile static and cyclic stresses in the presence of a nitric acid solution. The stress corrosion fracture process in the rods was monitored using acoustic emission techniques. The experimental loading conditions simulated possible in-service loads for composite suspension insulators. The results obtained in this study showed that the brittle fracture process can be generated in the rods when subjected to relatively low tensile stresses in the presence of a nitric acid solution. The morphology of the experimentally generated brittle fracture cracks in the rods closely resembles those from in-service failed composite suspension insulators. It has also been shown in this research that low frequency, low amplitude vibrations in tensile loads can significantly accelerate the fracture process. It appears that the brittle fracture cracks in the rods generated under cyclic loads are less planar in nature in comparison with the cracks formed under static conditions. It has also been found that the acoustic emission generated during the stress corrosion fracture process in the rods is sensitive to the placement of the transducers. However, a reasonably good correlation between the stress corrosion crack growth rates and acoustic emission has been attained.

1. Introduction

In recent years a great deal of development has been carried out on GRP (glass fiber reinforced polymer) composites for use as electrical insulators. Composite suspension insulators are used in overhead transmission lines with line voltages in the range 69 kV to 735 kV. These insulators (see Fig. 1) rely on unidirectional glass reinforced polymer composite rods as the principal load-bearing components. The rods are manufactured by pultrusion, and the constituents are either polyester, vinyl ester, or epoxy resins reinforced with either E-glass or ECR-glass fibers. The fibers are axially aligned and constitute 55 to 60% of the rod by volume. The surface of the GRP rod is covered with a rubber sheath with several weathersheds. The ends of the rods are supported by two metal end-fittings. One end-fitting (the energized end or the hot end) is attached to a high voltage line whereas the other end (the cold end) is attached to the tower. In order to reduce the electric stress concentrations at the energized end, grading rings are used on 115 kV lines and higher.

Reasons for the use of composite insulators in high voltage applications include: an exceptional high strength to weight ratio, improved damage tolerance, structural flexibility and greater impact resistance. However, the use of composite insulators is not without problems. The GRP composite materials present a significant problem in that they may fail by brittle fracture, which usually takes place in a catastrophic manner [1–6]. The observed failures usually occur under 5–10% of the load-bearing capacity in dry fracture. The fracture surface is typically very planar and large. On occasion the planar fracture surface can be as much as 80–90% of the cross section area of the rod [4].

Generally the brittle fracture of composite insulator rods is associated with high voltage applications. In a high voltage environment, acids, such as nitric acid, may be present or generated near the line insulators. The fact, that a nitric acid solution can be formed in-service has been speculated for some time. Recently, Chughtai *et al.* [6] have detected, using Fourier transform infrared spectroscopy, the presence of nitrate on the brittle fracture surfaces of a 115 kV suspension insulator which failed in-service by brittle fracture. This result implies that brittle fracture of suspension composite insulators can be caused by a nitric acid

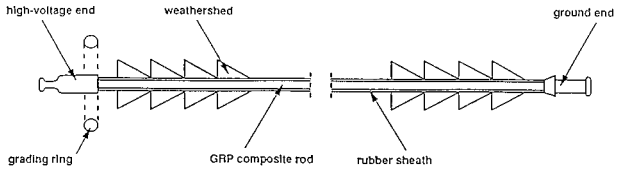

Figure 1 Schematic of a composite suspension insulator.

formed through corona discharges. Since corona discharges frequently occur in the immediate vicinity of the energized end-fittings of suspension insulators, oxides of nitrogen and nitric acid are formed in-the presence of ozone and moisture. Possible chemical reactions of the nitric acid formation process were given and discussed in Ref. 6. Another possible source of nitric acid is acid rain. A principal natural source of gaseous NO_x is generated from chemical decomposition of nitrides in the atmosphere. In addition, man made gaseous emissions are known to be heavily concentrated near population centers where large power lines are common.

Brittle fracture of composite insulators is caused by the stress corrosion cracking (SCC) of the composite rod material [1–6]. SCC in an E-glass/polymer composite results from the combined effect of low mechanical tensile stresses applied along the fibers and chemical attack of either organic or inorganic acids. With the presence of acids on the GRP materials, calcium and aluminum within the fiber are leached out by ion exchange with hydrogen [7–10]. The leachibility of these metallic ions is not only determined by the hydrogen ion concentration but also strongly affected by the anions in acids.

Constant K_I samples have been designed and used to test the stress corrosion properties of unidirectional E-glass fiber/polymer composites under static loads [8, 11, 12]. The brittle fracture process in unidirectional E-glass/polymer composite materials has been reproduced under laboratory conditions by subjecting the K_I specimens to very low mechanical loads in the presence of various corrosive environments [1–3]. The stress corrosion experiments were performed with the specimens immersed in either organic (oxalic acid) or inorganic acids (nitric and hydrochloric acids). In addition, the brittle fracture process has been initiated in the specimens subjected to corona discharges in the presence of small amounts of water [1–3].

The morphology of the fracture surfaces in the K_I specimens has been found to be highly dependent on the value of K_I [1–3, 8]. For low values of K_I the surfaces are always planar in nature and perpendicular to the fibers. Higher values of K_I generate surfaces which are less planar with numerous steps or ridges on the crack surface. The crack propagation rates during the stress corrosion fracture process in the K_I specimens can be determined by monitoring acoustic emission [11, 12].

In this study, an attempt was made to initiate brittle fracture in the GRP rods under the conditions which would be similar to the in-service loading conditions of composite high voltage suspension insulators. The acoustic emission generated during brittle fracture was also measured and characterized. There were a number of goals for the reported investigation: First (1), due to geometric similarity, it was hoped that the brittle fracture process in an actual composite insulator rod could be generated with conditions at least somewhat like those that might be encountered in-service. Second (2), assuming a successful generation of brittle fracture cracking, it would be important to monitor its development and determine if information about the involved fracture processes could be obtained. Third (3), it was important to examine both static and fatigue loading to establish if the brittle fracture mechanisms are the same in both of these loading arrangements. Fourth (4), it was hoped that the measurement of acoustic emission would provide insight into both the mechanisms of brittle fracture in the composite rods and to a possible technique for the prediction and detection of brittle fracture in composite insulators in-service.

2. Experimental procedures

Experiments were set up and carried out using several short composite insulators with rods 0.61 m (2 ft.) in length. Each insulator had two crimped metal end-fittings, no additional housing or weathersheds were used. The composite insulator rods were either held at a constant static stress or cycled in tension-tension fatigue at about the stress with a ±7–8% over and under load. The experimental conditions used are summarized below:

- Rod diameters: $d = 16$ mm (0.62 inch) and 19.4 mm (0.75 inch)
- Axial load stress: $\sigma = 130$ MPa (same for both diameter rods)
- static: Load = 26.1 kN small rod diameter and 38.4 kN large rod diameter
- cyclic conditions: Load = 26.1 kN, 8% overload, frequency 10 Hz., Load = 38.4 kN, 7% overload, frequency 10 Hz.
- Initial defects: Surface pre-crack: 10 mm in length, 0.3 mm in depth and 0.1 mm in thickness. No surface crack, but an opening in the rubber coating about 1 mm in height and 3 mm in width.
- Corrosive environment: Nitric acid, pH = 1.2

As noted above two types of surface defects were employed. In one case the initial precrack introduced on the rod surface within the acid exposure region was approximately 10 mm in length, and 0.3 mm in depth. The pre-crack was introduced to initiate a stress corrosion crack in one particular place on the rod surface. In the second case the rod was completely covered with silicon rubber inside the acid tank except for a small opening about 1 mm in height and 3 mm in width.

In all tests a liquid nitric acid environment was used with a pH of 1.2. The acid was held in a 125-ml container sealed around the rod. To prevent the acid from leaking out due to potential debonding along the rod, the rod, from the container to the bottom end fitting, was coated with silicon rubber. Three wide band acoustic emission transducers (B1025, Digital Wave) were located on or near the composite rod sample. One was

TABLE I Test conditions

Test condition	*d* (mm)	Axial Load (kN)	Stress (MPa)
Static	16	26.1	130
Static	19.4	38.4	130
Static*	16	26.1	130
Static**	16	9-13.6	43
Static + 7%	19.4	38.4 + 7%	130 + 7%
Fatigue (10 Hz)	16	26.1 ± 8%	130 + 8%
Fatigue (5 Hz)	19.4	38.4 ± 7%	130 ± 7%
Fatigue (10 Hz)	19.4	38.4 ± 7%	130 ± 7%
Fatigue (20 Hz)	19.4	38.4 ± 7%	130 ± 7%

*/** For * test, there is no surface pre-crack, but there is a 1mm in height and 3 mm in width opening on the silicon rubber cover. For ** test, there is about 3 mm in diameter opening in the silicon rubber cover and a hole in the rod 2 mm in depth. For all other tests, there is a 10 mm surface pre-crack.

hung in air near the top coupling to monitor noise in the lab area. The second was located directly behind the pre crack or defect, just above the acid (called the opposite transducer). The third transducer was located at the same height but 90° around the rod from the second transducer (called the side transducer). The acoustic emission was measured by a standard PC controlled parameter measuring system (Phoenix system). Schematic diagrams of the test setup and the initial defects are shown in Figs 2 and 3. Table I provides a summary of the test conditions employed in the stress corrosion experiments.

The rods tested in this study were unidirectional E-glass/modified polyester composite materials with a volume fraction of fibers at approximately 0.55 (0.72 by weight). Both the design of the end-fitting and the exact composition of the polymer matrix are proprietary information.

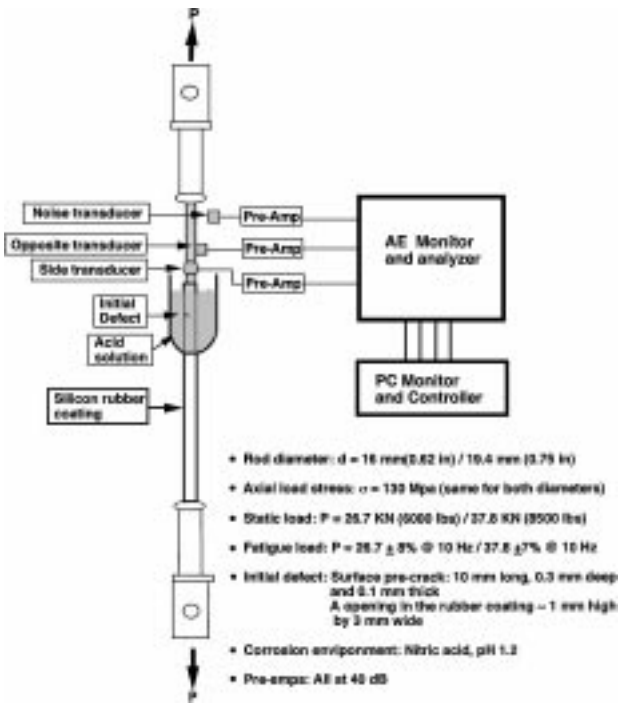

Figure 2 Experimental set-up used in the stress corrosion experiments.

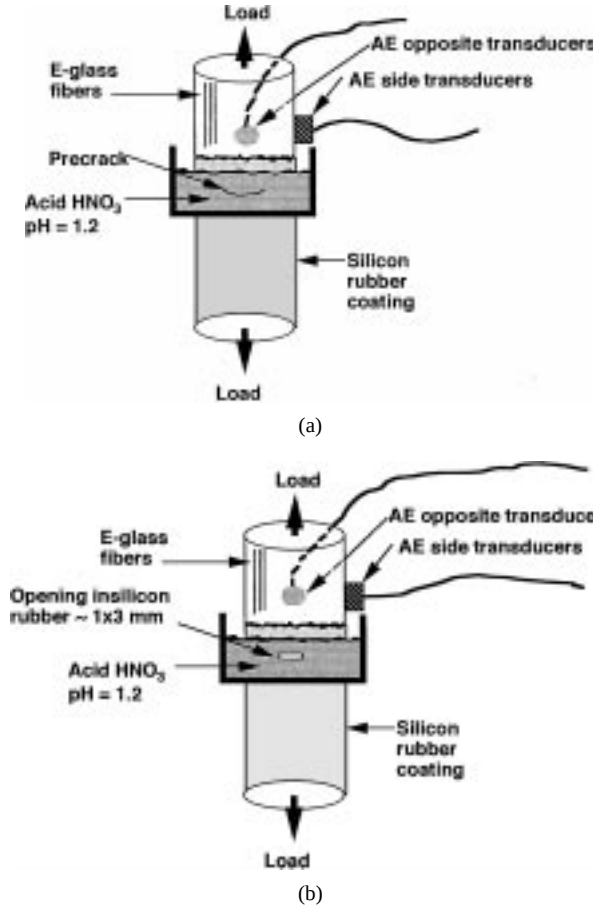

Figure 3 Surface conditions in the rod experiments; (a) GRP rod with a surface pre-crack, and (b) GRP rod coated with silicon rubber and a small opening.

3. Experimental results

3.1. Fracture surface morphology

The majority of tests (constant static stress and cycling) with a small pre-crack failed in a brittle fracture manner. The crack advanced in a flat planar manner for some distance in the direction perpendicular to the fibers and then long vertical splits occurred along the fibers. This process, crack advance then vertical splitting, was repeated until the sample essentially shredded and pulled apart. The details of fracture and fracture face morphology will be discussed in detail in the next section. However, a small number of samples (two samples) did not fail in this manner. In these cases, multiple surface cracks were formed on the rod surface and they continued to grow around the outside of the test specimen. Fig. 4 shows an example of these cracks. No significant planar crack growth was observed at the pre-crack for these two specimens.

The fracture faces obtained from brittle fracture due to static loading with a pre-crack and those obtained from cycling loading with a pre-crack were found to be quite different. The fracture surfaces resulting from the different types of loading could easily be distinguished from one another. In both cases, if there was a planar pre-crack, the crack continued to grow in a planar fashion until vertical splitting along the outside of the rod occured. This same procedure (crack advance then vertical splitting) was repeated several times as the crack advanced. Finally, the sample failed by the splitting and

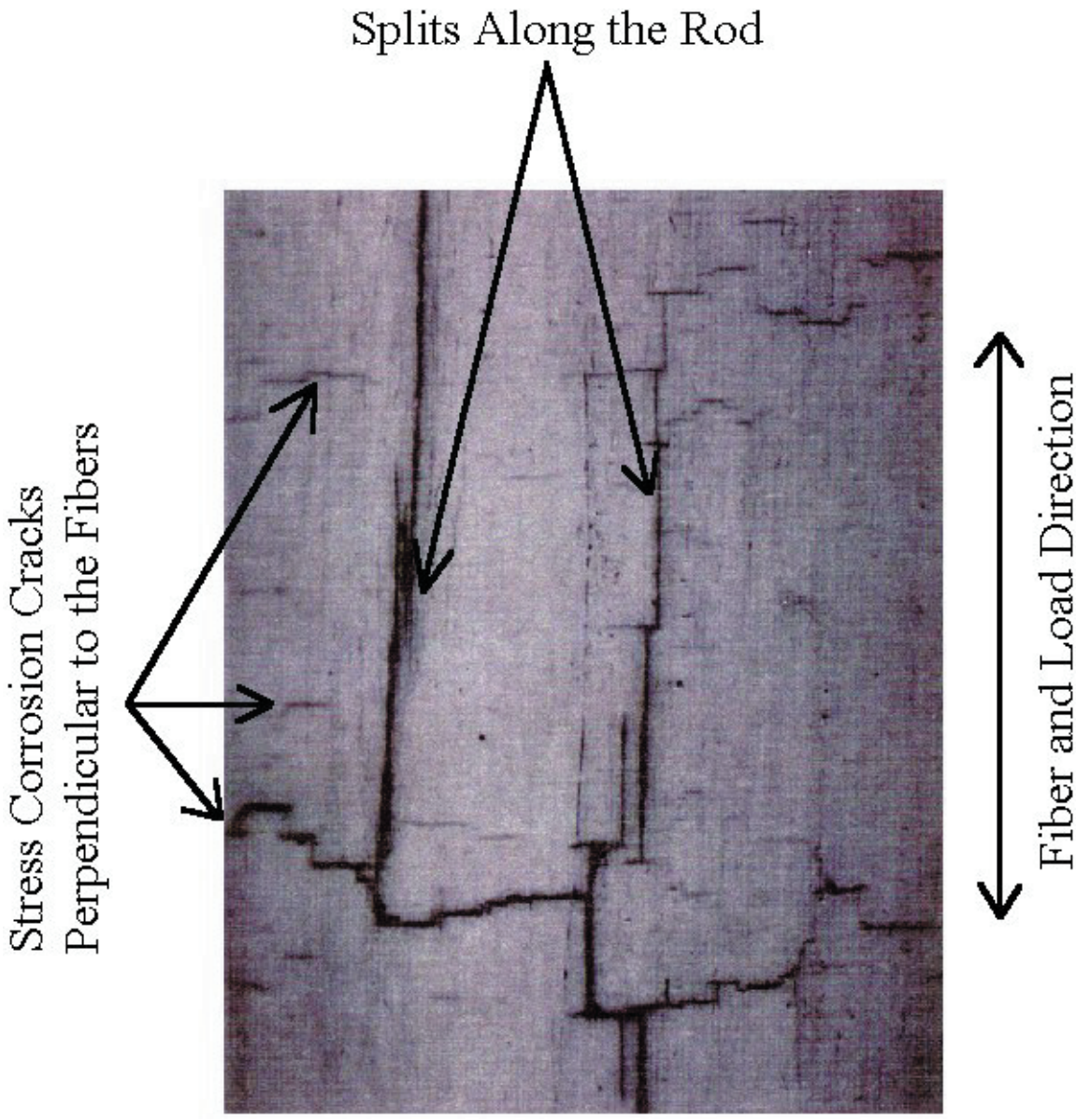

Figure 4 A network of brittle fracture cracks on the surface of the GRP rod tested under static conditions with a load of 26.1 kN.

pull out of long strands of the composite rod. This failure process was duplicated several times for both static and cyclic loading. The published tensile strength of the E-glass fiber/polyester composite is approximately 700 to 1000 MPa [13] yet the failures observed when exposing the rod to nitric acid can occur at stresses below 130 MPa. Clearly, the presence of the acid is a major factor in the brittle fractures we observed. Stress corrosion crack mechanisms are the cause of the observed brittle fracture. Examples of the fracture surfaces for both static and cyclic failures are shown in Fig. 5, a–d.

In two of the tests, which also failed by brittle fracture, different fracture characteristics were observed. One sample was statically loaded to 130 MPa and all of the rod surface exposed to acid was covered with silicon rubber expect a very small (1 mm in height and 3 mm in width) opening in the rubber coating (see Fig. 3b). This sample failed in a brittle failure mode with the major difference being that the planar crack area was considerably larger and spreads out in a fan shaped manner from the hole in the rubber coating. A micrograph of this failure is shown in Fig. 6. Point A in Fig. 6 indicates the initiation place of the brittle fracture crack and the location of the initial acid attack on the composite. The other test was similar except a very small diameter hole (3 mm in diameter) was drilled through the silicon rubber and into the rod approximately 2 mm. In this test, the sample was loaded only to 43 MPa. This sample required many more hours of exposure until failure. The approximate time to failure for most samples was in the range 35–50 hours. This sample was loaded at 43 MPa for 385 hours. It was then loaded to a stress level of 60 MPa for 6 hours and an audible report was heard and vertical splitting was observed. It was then unloaded, examined and reloaded to 43 MPa for 96 additional hours and then increased in stress to 65 MPa. It was held at 65 MPa until failure (2 hours). The failure was similar to the failure of other statically loaded samples. Again, the major exception was that the first planar crack area was considerably larger.

Analysis of Fig. 5a–d shows that the first planar crack area is noticeably larger for the statically loaded

samples compared to the samples loaded under cyclic conditions. Notice also an increased amount of splitting and fracture steps in the fracture surface of the fatigue tests. The fatigue tests are also characterized by crack propagation completely around the circumference of the tested rod. Table II presents data on the individual fracture faces for different test specimens. Included in the table is the percntage area occupied by the first planar transverse crack. This data is plotted in Fig. 7. Notice that the samples with no pre-crack and the ones tested at very low stress have significantly larger first planar areas. Another observed difference is the planar crack observed when there is no pre-crack. Here, the planar area spreads out from a point, giving what looks like a fan shaped crack (see Fig. 6).

Static overload tests were carried out to determine if the difference between the static and cyclic tests was due to the higher stresses obtained in the fatigue tests.

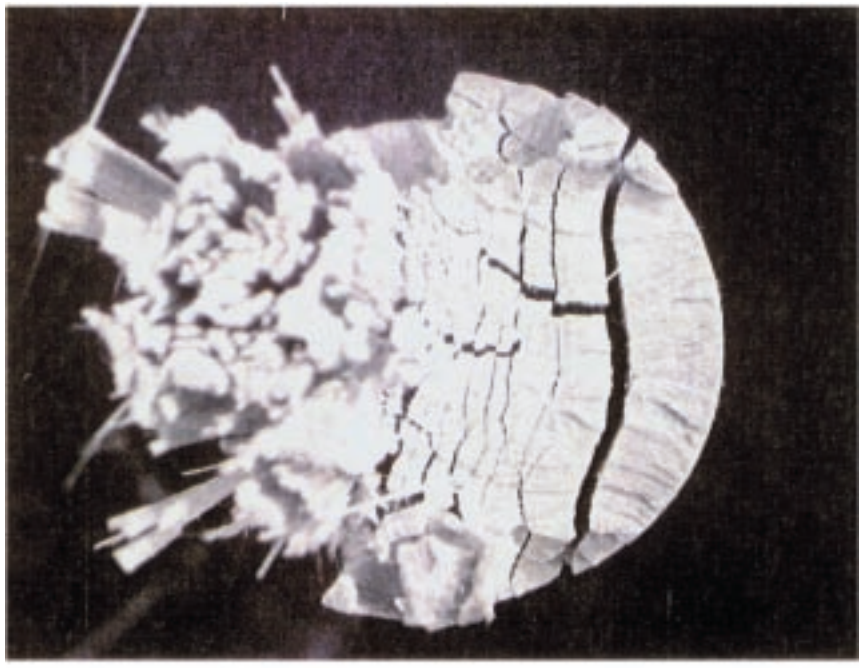

(a)

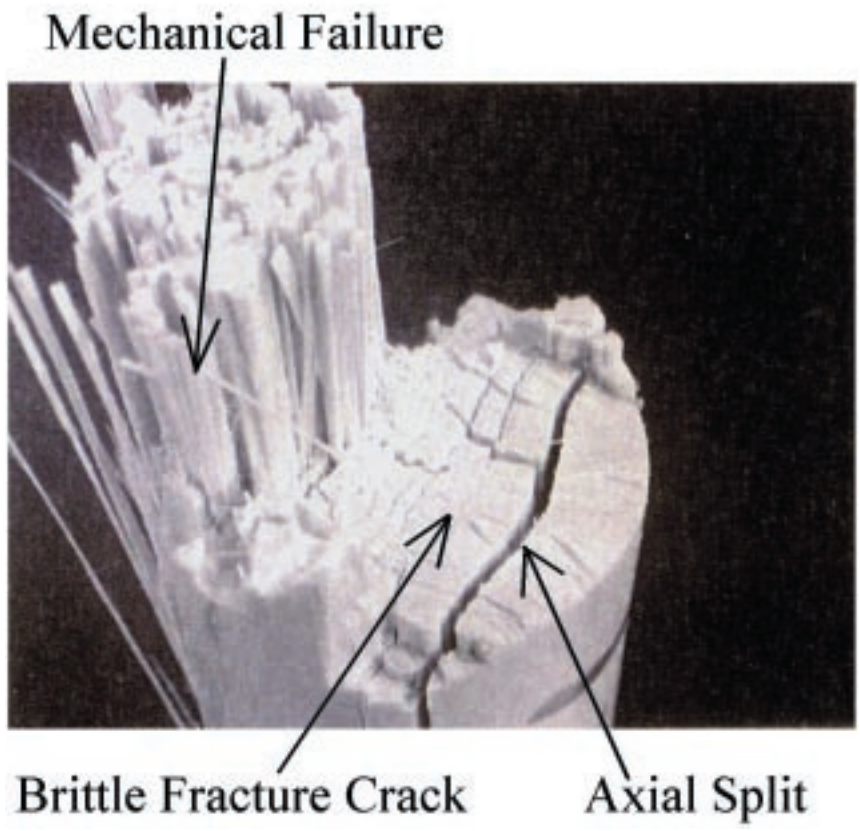

(b)

Figure 5 Brittle fracture damage zones in the GRP rods with a rod diameter of 19.4 mm; (a, b) under static conditions (38.4 kN load) and (c, d) under cycling conditions (38.4 kN ± 8%, 10 kz). (*Continued*)

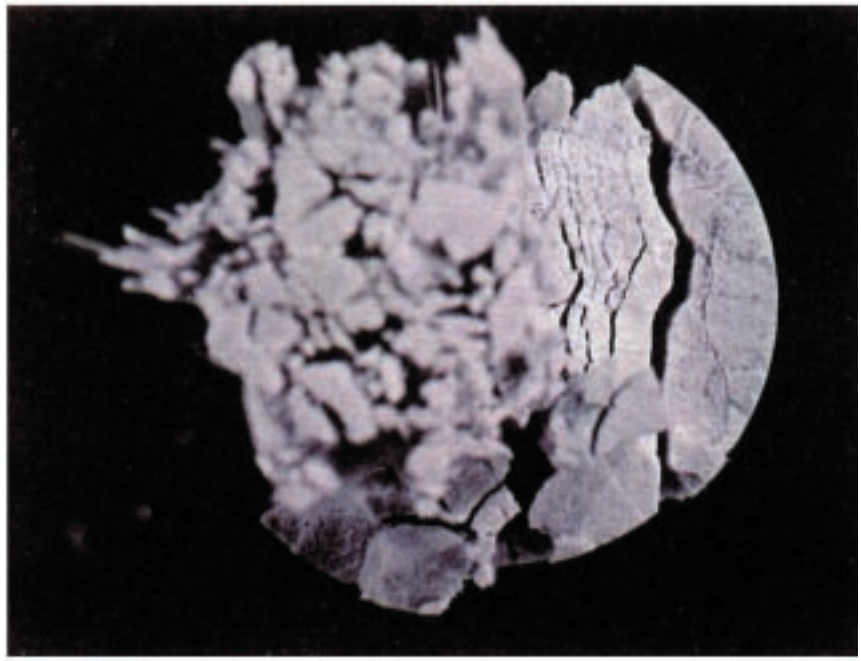

(c)

(d)

Figure 5 (*Continued*).

The tests were performed at a stress level equal to the highest stresses obtained in the cyclic experiments. The resulting fracture faces obtained from the over load tests were identical to the fracture faces from the previous static tests. The differences in morphology were not due to stress but to other mechanisms related to the cyclic loading conditions. This will be discussed in the next section of the paper.

For both the static load and cyclic tests, from the initialization of the pre-crack until the final failure, (see Figs 5a–d, and 6) the fracture surface changes from a planar surface to an irregular surface (with multiple steps) and then to a fiber pull out and multiple mechanical failures of the fibers.

3.2. Acoustic emission monitoring

Acoustic emission is the rapid release of energy due to a sudden localized change of stress or strain. The fracture of a fiber should be an excellent source of

TABLE II Planar crack area from surface pre-defect to first splitting

Rod Diameter, (mm)	Load, (kN)	Stress, (MPa)	Defect, (mm)	Distances to vertical splitting, (mm)	Area, (to 1st split), $(mm)^2$)	Area %
16	static 26.1	130	pre-crack 10	4, 7, 8, 9	39.3	19.6
16	static 26.1	130	no defect	5, 7, 9	53.7	26.7
16	static 9 ~ 13.6	43	3 mm dia. hole ~2 mm deep	5.6, 9, 11	61.2	30.4
19	static 38.4	130	pre-crack 10	4, 6, 7.7	44.0	14.9
19	static 26.1 + 7%	130 + 7%	pre-crack 10	4.5, 6.5, 8	52.0	17.6
16	fatigue 26.1 ± 8%, 10 Hz	130 ± 8%	pre-crack 10	2, 3.5, 4	14.5	7.2
19	fatigue 38.4 ± 7%, 5 Hz	130 ± 7%	pre-crack 10	2, 3	16.1	5.4
19	fatigue 38.4 ± 10%, 10 Hz	130 ± 7%	pre-crack 10	2, 3.5, 5	16.1	5.4
19	fatigue 38.4 ± 7%, 20 Hz	130 ± 7%	pre-crack 10	1.5, 2, 4.5	10.5	3.6

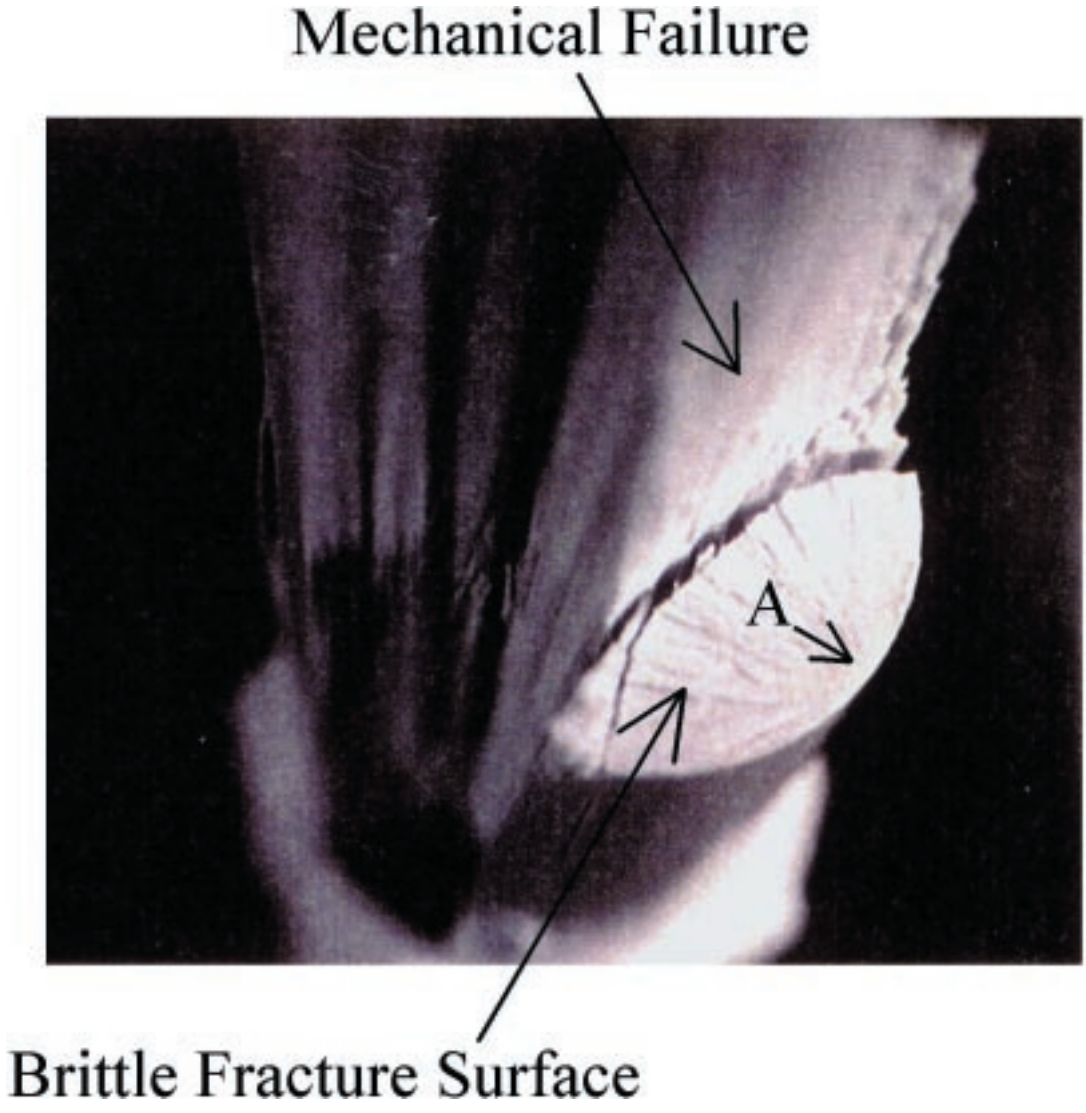

Figure 6 Brittle fracture surface from the stress corrosion experiment on a 16 mm diamter rod with an opening in the rubber coating without a surface pre-crack and a static load of 26.1 kN.

acoustic emission as well as splits and matrix cracking. The emissions are recorded and measured from the electrical signal produced by a piezoelectric disk in the transducers, which were placed on the composite rod a short distance from the failure zone. During the tests reported in this paper, the number of acoustic emission signals and their peak amplitude have been monitored and measured throughout the entire time of each test. The specimens were loaded into an 880 MTS deformation machine and loaded at the rate of 4.5 kN/min. until the desired stress was reached. At this point, the transducers were attached, acid was placed in

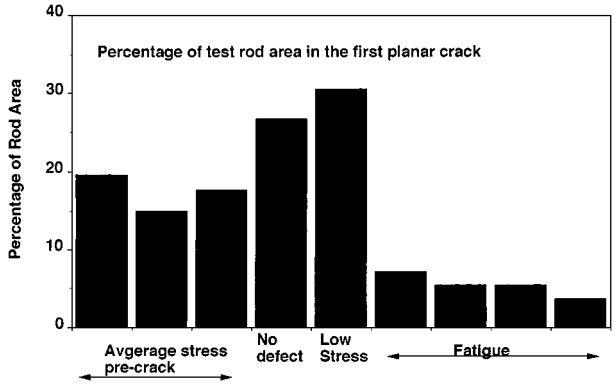

Figure 7 Brittle fracture surfaces (percentage of the rod surface in the first planar crack) generated in the static (with and without overload) and cyclic stress corrosion experiments.

the container being certain to cover the initial defect and then monitoring of the acoustic emission was started. Due to the long duration of these tests extraneous laboratory noise was a significant problem which had to be measured. A third transducer used to measure laboratory noise was positioned near the other transducers but not attached to the sample. Signals registering on all three transducers at identical times were considered noise and were subtracted from the acoustic emissions measured on the side and opposite transducers.

The acoustic emission behavior was somewhat different from test to test. However, when a good planar crack was obtained, the sum of the acoustic emission signals produced a distribution with time similar to that shown in Fig. 8. The data are characterized by very little or no emissions for a significant length of time (approximately 15–25 hours) and then a rather sudden and large increase in the acoustic emission rate. The appearance of the increase in acoustic emissions was similar in test time for the majority of the samples tested. After the sudden increase, the rate of acoustic emissions slows considerably and maintains a slow constant increase for a lengthy time and then increases rapidly and maintains high activity until the sample fails. Fig. 9 shows the first increase in acoustic emission plotted as the rate of emissions rather than the sum. One factor is evident in both

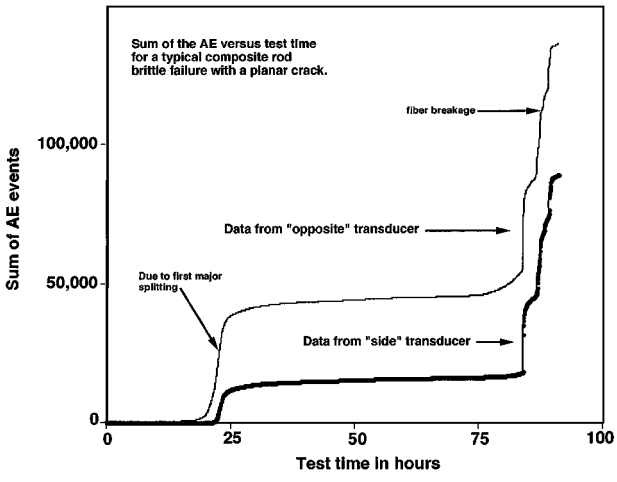

Figure 8 Sum of the acoustic emission events versus test time for a typical composite rod brittle failure monitored with the side and opposite transducers.

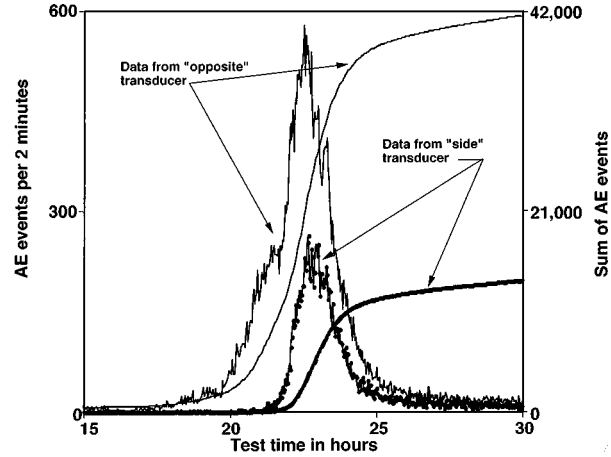

Figure 9 Rates of acoustic emission versus time from the transverse crack and the first split along the fibers.

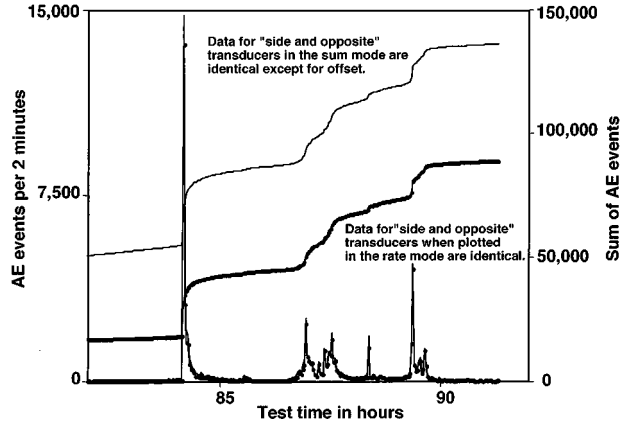

Figure 10 Rates of acoustic emission versus time from the final stages of the brittle fracture process in the GRP rod from both the opposite and side transducers.

Figs 8 and 9, the opposite transducer is more sensitive to the emissions generated than the side transducer for the first part of the test. However, after the first increase in acoustic emission the side and opposite transducers give essentially identical data. Fig. 10 shows the acoustic emission rate for both transducers during the final failure of the sample. Notice that the data from the two transducers is essentially identical for this time interval. The first peak in acoustic emission corresponds to the first appearance of vertical splitting along the fibers.

4. Discussion

Brittle fracture of composite suspension insulators is a rare phenomenon. It can occur if the insulators are not protected against moisture ingress into their end-fittings [2–5]. During the brittle fracture process, transverse cracks are formed in the GRP rods in the direction perpendicular to the fibers either inside or outside of the end-fittings. The most likely cause of the brittle fracture failures of suspension composite insulators is the formation of nitrides and nitric acid due to corona activities in the presence of moisture [6]. Nitric acid solutions can be formed externally on the surface of the fitting, weathersheds and the rubber sheath. If the acid

penetrates into the fitting, brittle fracture will occur inside the hardware (see Fig. 11) [4]. Nitric acid solutions can also be formed inside the insulators, above the fitting due to internal partial discharge inside the insulator if moisture is present. In this case, the GRP rod fails above the fitting (see Fig. 12) [4]. The location of the brittle fracture cracks with respect to the fitting depends strongly on the voltage level and the position and geometry of the grading rings [4, 5]. Despite the fact that the brittle fracture cracks inside and outside the fittings are planar in nature, there is a significant difference in the morphology of the fracture surfaces on the microscale. For the cracks inside the fittings, the surfaces of the failed fibers and the matrix are at the same level. For the external brittle fracture surfaces, the fibers are always sticking out above the surface of a polymer resin [1–5] with the matrix significantly decomposed, most likely by internal discharges.

The stress corrosion cracks generated in this study closely resemble the geometry of the cracks of the field failed insulators. Since the tests were conducted in a nitric acid solution (without corona discharges), no resin decomposition on the fracture surfaces was observed. Therefore, the stress corrosion experiments simulated very accurately the formation of brittle fracture cracks inside the fittings. It can be seen in Figs. 5 and 6 that the morphology of the fracture surfaces generated in the experiments with the very shallow pre-cracks and the opening in the silicon rubber are rather different. When the entire surface of the rod was exposed to the acid, a series of steps was noticeable on the fracture surfaces. In the second case, fan shape surface marks are visible (see Fig. 6) emanating from the area where the acid was attacking the composite rod (from the opening). It can therefore be concluded that the crack in the first case was growing along the entire front of the precrack whereas in the second case the fracture process was initiated on the rod surface inside the opening. Both types of the fracture surfaces have been observed in several field-failed composite insulators [2–5]. In some cases a single brittle fracture will not be initiated [2, 3]. Instead, a network of cracks will be formed on the rod surface similar to the surface damage shown in Fig. 4. Since the failure of the insulators above the fitting is caused by the formation of nitric acid solutions usually at the rod/rubber sheath interface above the hardware, a large portion of the rod surface can be exposed to the acid. Under these conditions, the surface damage will

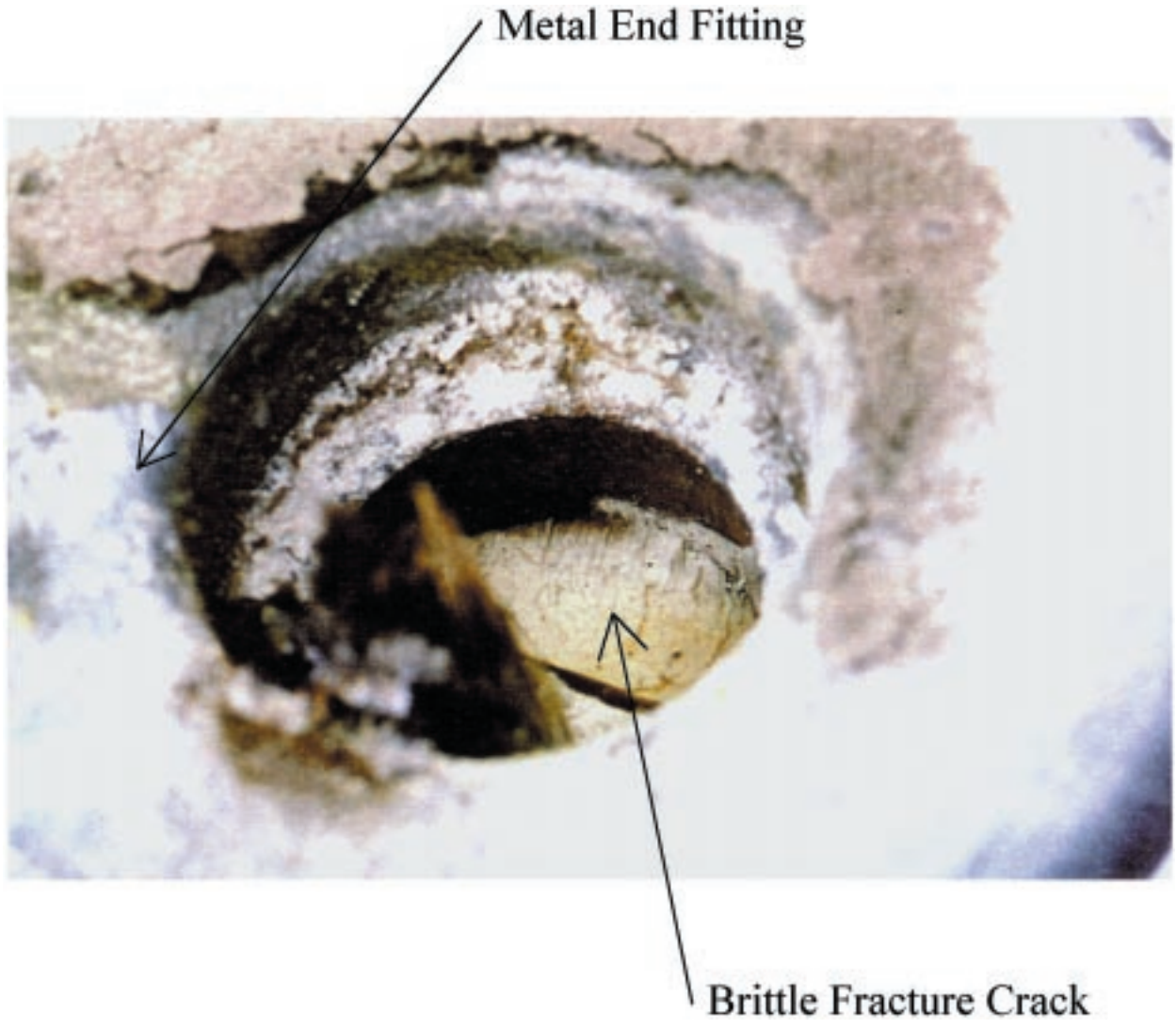

Figure 11 Brittle fracture of a 500 kV suspension composite insulator inside the fitting after approximately four years in-service with an applied load of 38 kN.

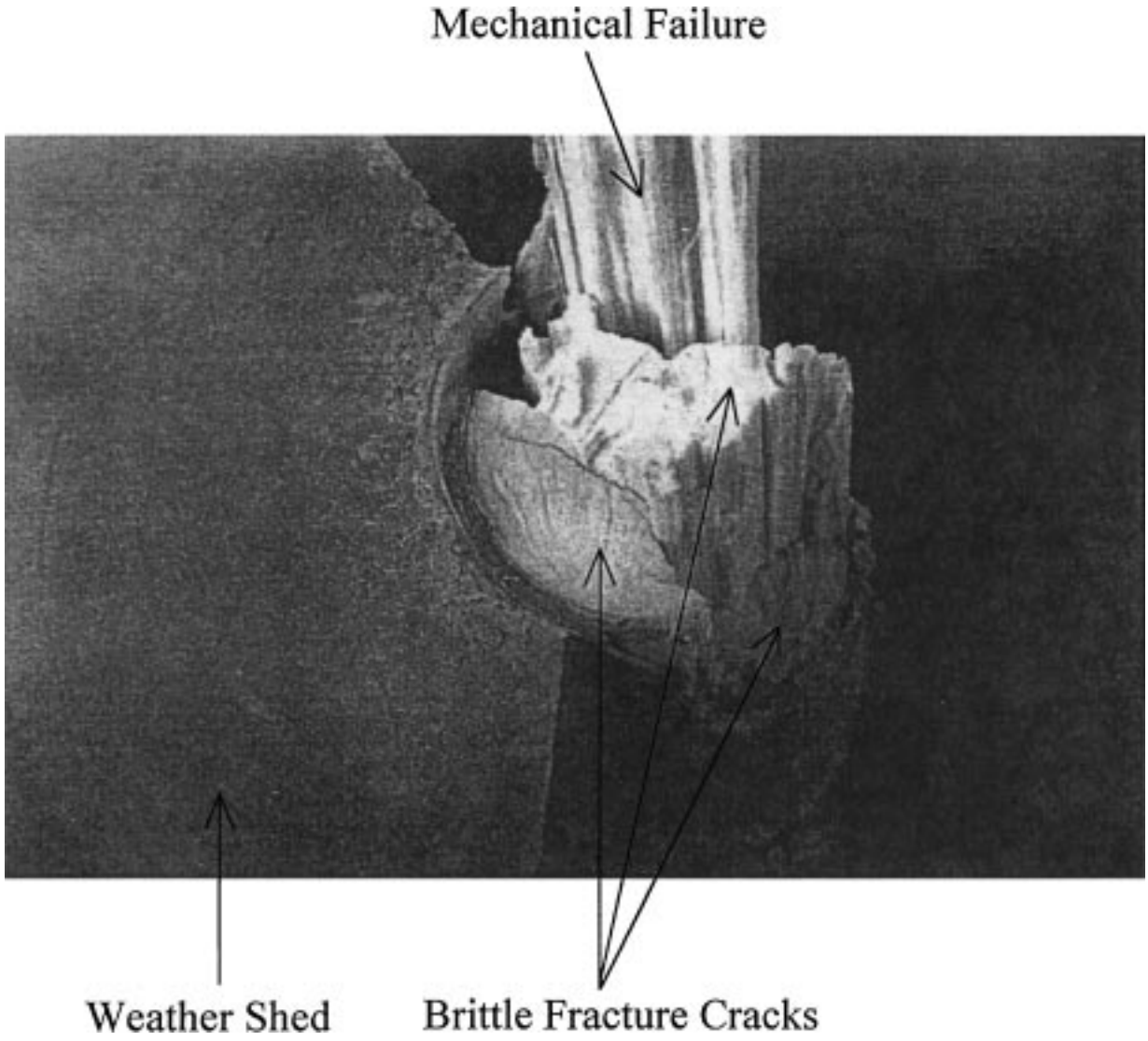

Figure 12 Brittle fracture of a 500 kV suspension composite insulator outside the fitting after approximately four years in-service with an applied load of 38 kN.

be generated with several brittle fracture cracks growing in the rod simultaneously. It is still unknown which factors determine the initiation of either a single brittle fracture crack or a network of cracks. Most likely, this is related to the surface imperfections on the rod surfaces. The critical surface flaw sizes for the initiation of brittle fracture cracks on the rod surfaces are unknown, and need to be investigated.

The main purpose of the stress corrosion experiments on the GRP rods was to reproduce the brittle fracture process in the insulator rods under the conditions which could be similar to in service conditions. Moreover, an attempt was made in this study to design a stress corrosion experiment using a specimen geometry which was closer to the actual geometry of a composite insulator. Most of the stress corrosion research performed in the past regarding brittle fracture [1–3] concentrated on the stress corrosion experiments in E-glass/polymer composite rod materials using the constant K_I specimens. The specimens were subjected to small applied tensile loads in the presence of various corrosive environments such as water as well as organic and inorganic acids. In addition, high voltage fracture experiments were also conducted by subjecting the mechanically loaded constant K_I specimens to corona discharges in the presence of small amounts of water. When stress corrosion cracks developed in the specimens under the above conditions, the brittle fracture process was monitored using acoustic emission. In the case of the K_I tests, the application of acoustic emission was very successful [1–3, 11, 12].

The growth of brittle fracture cracks has been successfully monitored using acoustic emission [1–3, 11, 12]. In particular, acoustic emission was used to determine the rate of stress corrosion crack growth by counting the fibers fracturing during the process. A one-to-one relationship between the number of the fractured fibers on the corrosion fracture surfaces and the number of acoustic emission signals from the fibers was established [11, 12]. The stress corrosion experiments on the GRP rods performed in this study, however, proved to be much more difficult. Contrary to the cracks in the K_I specimens, the exact length of the stress corrosion cracks in the rods could not be determined optically (for example using a traveling optical microscope). In addition, the stress conditions at the tips of the cracks in the rods and the K_I specimens were entirely different. The macro-stress conditions in the K_I specimens did not depend on the crack length

for a given applied tensile load. In the rods, however, the stress intensities at the tips of the cracks growing perpendicular to the fibers increased as a function of crack length and their geometry for a constant applied tensile load [5]. Since the nature of the brittle fracture process strongly depends on the stresses at the crack tip, and thus, the value of the stress intensity factor K_I, the stress corrosion process changes as the crack propagates perpendicular to the fibers across the rod. What is still very surprising is the fact that the stress corrosion cracks in the rods are so large. An unsuccessful attempt has been made by Kumosa *et al.* [5] to explain this very unusual phenomenon by performing three-dimensional finite element simulations of the stress corrosion cracks in homogenous orthotropic linear elastic rods. Due to the obvious limitations of the finite element analysis the numerical results and the critical stress intensities for debonding (taken from the constant K_I stress corrosion experiments) did not explain why the cracks are so large. The finite element modeling (FEM) showed that the cracks should be significantly smaller (less than 5% of the rod cross section) for a load of 27 kN. Since the static stress corrosion experiments performed on the smaller rods ($d = 16$ mm) were very close to the conditions in the FEM model, this further reinforced the conclusions in Ref. 5 about the invalidity of the finite element computations.

The acoustic emission generated during the brittle fracture of composite insulator rods is generally characterized by a peak in the acoustic emission rate at 15–20 hours after the start of the test. The acoustic emission then increases slowly for many hours and then increases rapidly and maintains a high level of activity until final failure occurs. It is believed that the first increase in acoustic emission is related to the growth of a transverse crack from the initial pre-crack until perpendicular splitting of the rod occurs. A visual correlation of the occurrence of the perpendicular splitting during and just after the acoustic emission increase has been observed in the laboratory. There is a linear correlation between the planar crack area and the number of acoustic emission signals measured until the beginning and the end of the first increase. Fig. 13 shows a plot of the sum of the number of acoustic emission signals up to the first vertical splitting versus the percent of the rod covered by the planar crack to the first vertical splitting, for tests in which good data was obtained. The results shown in Fig. 13 clearly demonstrate that the crack propagation perpendicular to the fibers generates acoustic emission with the sum of events proportional to the size of the first transfer brittle fracture crack. Knowing the density of fibers within the composite, it is possible to estimate the number of fractured fibers in the first planar crack area. If we compare the sum of acoustic emission events, without the signals from the first peak, the total number of signals is several times lower than the number of fractured fibers on the planar fracture surface before splitting. However, if the data in the first peak are included the sum of acoustic emission is approximately four times larger than the number of fractured fibers estimated from the size of the cracks and the volume fraction of fibers. In the initial stages of

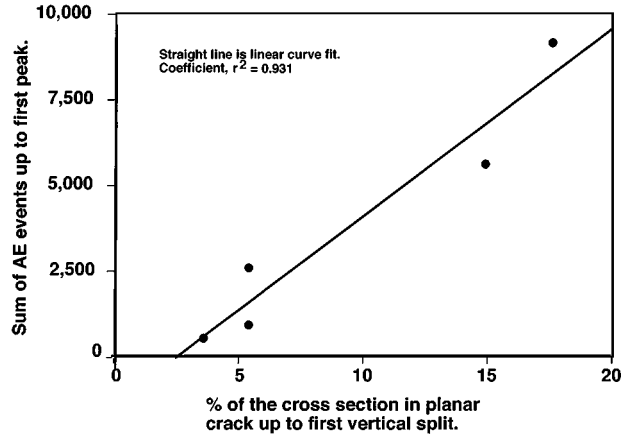

Figure 13 Sum of the acoustic emission events versus the area of the first transverse brittle fracture crack (up to the first vertical split) from the stress corrosion cracking in the GRP rod tested under static condition.

the crack propagation process acoustic emission significantly "underestimates" the number of fractured fibers, and thus, the crack propagation rate perpendicular to the fibers. This is not surprising since the acoustic emission monitored during the stress corrosion process in the rods appears to be strongly dependent on the transducer position with respect to the crack. Depending on the position of a fractured fiber at the crack tip with respect to the transducers, the sensitivity of acoustic emission changes. This means that for some fibers, acoustic emission will not be detected depending on their location on the fracture surface. Moreover, small transverse cracks will not release significant amounts of energy at fracture since the stress at the tip of a short transverse crack is not high. When splitting along the rod occurs, the transverse crack is already long with a relatively high crack propagation rate. At this point, the number of recorded acoustic emission signals is significantly larger than the number of fractured fibers. These additional signals are most likely due to matrix cracking, interfacial cracks formed during splitting and reflections of the signals from the top and bottom surfaces in the rod.

A complete understanding of the sensitivity of the transducer placement will require an understanding of wave propagation along a cylindrical rod. It appears that once vertical splits are formed on the rods surface, the difference in sensitivity is lost. Additional work is currently underway to understand and determine the cause of this behavior.

The effects of cyclic loading conditions on the failure of glass fiber/polymer unidirectional composites have been investigated by several researchers [14–16]. In particular, Cartis [15] studied the effect of load cycle tensile fatigue (10 Hz) on the failure properties of an E-glass fiber/epoxy composite. It was concluded in that study that splitting along the fibers was the primary damage growth mechanism. Similar observations were made by El Kadi and Ellyin [16]. This might explain the difference in the morphology of the fracture surfaces in the rods generated under static and cyclic loading conditions. Since the splitting formation along the fiber/matrix interfaces is more likely in fatigue, more

steps will develop on the stress corrosion fracture surface. It is apparent from the results presented in Fig. 7 that the effect of low frequency cyclic tension/tension fatigue is significantly stronger on the stress corrosion fracture process in the rods than the effect of the overload. An increase in the applied tensile loads on the rods by 8% did not result in a noticeable change in the morphology of the fracture surfaces. It can therefore be concluded that low frequency low amplitude tension/tension fatigue can significantly alter the nature of the brittle fracture process in composite suspension insulators. The cyclic loading conditons in the stress corrosion experiments on the E-glass/polyester rods simulated the possible vibrations of the conductors (aeolian vibrations) and suspension insulators caused by small winds [17].

The stress corrosion experiments on the GRP rods were performed under the conditions which could exist in-service. The mechanical loads applied to the insulators were very similar to the in-service loads caused by the weight of transmission lines. For example, a 345 kV insulator with the rod diameter of 16 mm can be subjected to loads up to 27 kN. This is the load which was used in the rod experiments. Moreover, the tension/tension fatigue conditions applied in the testing simulated typical low frequency, low magnitude aeolian vibration of high voltage transmission lines [17]. The methods of exposing the rods to the nitric acid solution also simulated possible in-service conditions at failure. The only factor which is still unknown and was assumed in the stress corrosion experiments a *priori* is the concentration of the nitric acid solution. The exact nitric acid concentration during the brittle fracture process in a composite insulator is still unknown. The fact that nitric acid is responsible for the brittle fracture failures has been shown by Chughtai *et al.* [6]. Most likely, the acid concentration during the process is not constant and varies with time. The critical acid concentration necessary to initiate the stress corrosion mechanisms for the E-glass/modified polyester composite from the K_I experiments has been determined to be approximately a pH of 3 [2, 3]. The acid used in the rod experiments was significantly stronger (pH of 1.2). This was done to accelerate the fracture process. However, it can be assumed that weaker nitric acid solutions will not change the morphology of the brittle fracture surfaces in the rods. They will only extend the time to failure of the rods.

5. Conclusions

Brittle fracture of composite insulator rods can be repeatably obtained in controlled laboratory conditions. Brittle fracture can be generated by either static or cyclic loading in a liquid nitric acid environment. The crack morphology of the brittle fracture damage zones in the rods is distinctly different for static loading and cyclic loading. The difference obtained are due to the fatigue and not due to the stress overload that occurs in fatigue. The main difference in the crack morphology is the size and depth of the first transverse planar crack. The crack is much larger for static loading than it is for cyclic loading. Other minor differences in crack morphology also occur as discussed earlier. The application of acoustic emission for the monitoring of stress corrosion cracking in the rods has been partially successful. Good correlation between the number of acoustic emission signals from the transverse crack propagation process and the size of the planar crack has been shown. However, a precise monitoring of the process by counting individual fibers from acoustic emission signals has not been possible. Moreover, the acoustic emission generated during the brittle fracture process in the composite rods seems to be strongly dependent on the position of the AE transducers.

Acknowledgements

This research was jointly sponsored by the Electric Power Research Institute under contract W08019-12 and a consortium of utilities consisting of the Bonneville Power Administration (96B194585), Western Area Power Administration (DE-FC65-96WA13221), Alabama Power Company (AP-0000-31287), Pacific Gas & Electric (4600001625) and the National Rural Electric Cooperative Association (95-15).

References

1. M. KUMOSA, Q, QIU, E. BENNETT, C. EK, T. S. McQUARRIE and J. M. BRAUN, in Proc. Fracture Mechanics for Hydroelectric Power Systems, edited by G. S. Bhuyan and J. Kibblewhite, Vancouver, BC, Canada, September 1994, p. 235.
2. M. KUMOSA, Q. QIU, M. ZIOMEK-MONOZ and J. M. BRAUN, Final Report to the Bonneville Power Administration, Western Area Power Administration, and the Electric Power Research Institute, Oregon Graduate Institute of Science & Technology, Portland, Oregon, 1994.
3. Q. QIU, PhD thesis, Oregon Graduate Institute, Portland, Oregon, 1995.
4. M. KUMOSA and Q. QIU, Final Report to Pacific Gas & Electric Company, Department of Engineering, University of Denver, May 1996.
5. M. KUMOSA, H. S. NARAYAN, Q. QIU and A. BANSAL, *Composites Science and Technology* **57** (1997) 739.
6. A. R. CHUGHTAI, D. M. SMITH and M. KUMOSA, *J. Composites Science and Technology* **58** (1998) 1641.
7. J. F. MANDELL, D. D. HUANG and F. J. McGARRY, *Composites Technology Review* **3**(3) (1981) 96.
8. D. HULL, M. KUMOSA and J. N. PRICE, *Materials Science and Technology* **1** (1985) 177.
9. B. DAS, B. D. TUCKER and J. C. WATSON, *J. Mater. Sci.* **26** (1991) 6606.
10. Q. QIU and M. KUMOSA, *Composites Science and Technology* **57** (1997) 497.
11. M. KUMOSA, D. HULL and J. N. PRICE, *J. of Materials Science* **22** (1987) 331.
12. M. KUMOSA, *J. Phys. D: Appl. Phys.* **20** (1987) 69.
13. D. HULL, "Introduction to Composite Materials" (Cambridge Press).
14. M. F. HORSTEMEYER and G. H. STABB, *Journal of Reinforced Plastics and Composites* **9** (1990) 446.
15. P. T. CURTIS, *Int. J. Fatigue* **13**(5) (1991) 377.
16. H. ELKADI and F. ELLYIN, *Composites* **25**(10) (1994) 917.
17. O. PERKINS, Western Area Power Administration, private communication.

Received 26 February 1998
and accepted 9 December 1999